Journal of Pathology
J Pathol July 2024; **263:** 328–337
Published online 17 April 2024 in Wiley Online Library
(wileyonlinelibrary.com) DOI: 10.1002/path.6286

ORIGINAL ARTICLE

ΔNp73 and its effector targets promote colorectal peritoneal carcinosis and predict survival

Daniel Pastor-Morate[1], Lidia Amigo-Morán[1], María Garranzo-Asensio[2], Raquel Rejas-González[2], Patricia Carnicero[1], Nuria Rodríguez[3], Juan Pedro Pérez-Robledo[4], Rodrigo Barderas[2], Isabel Prieto-Nieto[4*†] and Gemma Domínguez[1*†]

[1] *Department of Medicine, Faculty of Medicine, "Alberto Sols" Biomedical Research Institute, CSIC-UAM and IdiPAZ, Madrid, Spain*
[2] *Carlos III Health Institute, Functional Research Unit into Chronic Diseases (UFIEC), Madrid, Spain*
[3] *Department of Medical Oncology, La Paz University Hospital, IdiPAZ-UAM, Madrid, Spain*
[4] *Peritoneal Carcinosis Unit, Department of General and Gastrointestinal Surgery, La Paz University Hospital, IdiPAZ-UAM, Madrid, Spain*

**Correspondence to: I Prieto-Nieto, Hospital Universitario La Paz, Pº de la Castellana, 261, 28046 Madrid, Spain. E-mail: iprieto@intermic.com; G Domínguez, Instituto de Investigaciones Biomédicas Alberto Sols, C/ Arturo Duperier, 4, 28029 Madrid, Spain. E-mail: gemma.dominguez@uam.es*

†These authors have contributed equally to this work as senior authors and are co-corresponding authors.

Abstract

Peritoneal metastasis of colorectal origin appears in ∼10–15% of patients at the time of diagnosis and in 30–40% of cases with disease progression. Locoregional spread through the peritoneum is considered stage IVc and is associated with a poor prognosis. The development of a regional therapeutic strategy based on cytoreductive surgery, and hyperthermic intra-abdominal chemotherapy has significantly altered the course of the disease. Although recent evidence supports the benefits of cytoreductive surgery, the benefits of hyperthermic intra-abdominal chemotherapy are, however, still a matter of debate. Understanding the molecular alterations underlying the disease is crucial for developing new therapeutic strategies. Here, we evaluated the involvement in peritoneal dissemination of the oncogenic isoform of *TP73*, *ΔNp73*, and its effector targets in *in vitro* and mouse models, and in 30 patients diagnosed with colorectal peritoneal metastasis. In an orthotopic mouse model, we observed that tumor cells overexpressing *ΔNp73* present a higher avidity for the peritoneum and that extracellular vesicles secreted by *ΔNp73*-upregulating tumor cells enhance their dissemination. In addition, we identified that tumor cells overexpressing *ΔNp73* present with dysregulation of genes associated with an epithelial/mesothelial-to-mesenchymal transition (MMT) and that mesothelial cells exposed to the conditioned medium of tumor cells with upregulated *ΔNp73* present a mesenchymal phenotype. Lastly, *ΔNp73* and its effector target RNAs were dysregulated in our patient series, there were positive correlations between *ΔNp73* and its effector targets, and *MSN* and *ITGB4* (*ΔNp73* effectors) predicted patient survival. In conclusion, *ΔNp73* and its effector targets are involved in the peritoneal dissemination of colorectal cancer and predict patient survival. The promotion of the EMT/MMT and modulation of the adhesion capacity in colorectal cancer cells might be the mechanisms triggered by *ΔNp73*. Remarkably, ΔNp73 protein is a druggable protein and should be the focus of future studies.

Keywords: *ΔNp73*; colon cancer; peritoneal metastasis; prognosis; survival; epithelial–mesenchymal transition; MSN; ITGB4; TP73

Received 5 December 2023; Revised 2 February 2024; Accepted 20 March 2024

No conflicts of interest were declared.

Introduction

Colorectal cancer (CRC) is the third leading cause of cancer worldwide and the second highest in mortality due to neoplastic diseases [1]. Approximately 15–20% of patients with CRC present metastasis at diagnosis [2]. Peritoneal involvement by the primary tumor defines peritoneal carcinosis (CRC-PC) and appears in ∼30–40% of cases with disease progression. Although CRC-PC is a locoregional disease, it is considered stage IVc [3] and is associated with a poor prognosis. The development of a therapeutic strategy with curative intent based on cytoreductive surgery (CRS) and hyperthermic intra-abdominal chemotherapy (HIPEC) [4] has significantly altered the course of this disease. Recent evidence supports the benefits of CRS; however, the benefits of HIPEC remain a matter of debate [5]. In this scenario, identifying the molecular mechanisms underlying CRC-PC is essential for identifying new targetable pathways.

Mutations in genes classically altered in CRC, such as *BRAF*, *KRAS*, *NRAS*, *PIK3CA*, *P53*, *SMAD4*, and *APC*, have been reported in patients with CRC-PC [6].

Somatic mutations in other genes, such as *ARID1A*, *PKHD*, *UBR5*, *PAX5*, *ASXL1*, and androgen receptor (*AR*) [7], have also been identified. Interestingly, CRC-PC has been defined as representing the molecular subtypes CMS4 and MSN [8], and the *CXCL2–CXCR2* signaling axis [9] plays a key role in peritoneal dissemination. Interestingly, areas with tumor metastases are enriched in cancer-associated fibroblasts (CAFs) that might be derived from resident mesothelial cells. These CAFs can secrete factors that favor the disorganization of the peritoneum, making it more accessible for tumor cells [10]. Despite these findings, further studies are required to identify key players of the disease that might be druggable.

The TP53 family plays a critical role in the initiation and progression of most tumor types [11]. In CRC-PC, TP53 is associated with adverse prognostic factors [6]; however, the involvement of other variants of the family has not yet been analyzed. ΔNp73 is an oncogenic isoform of the TP53 family member TP73 that results in the loss of the amino-terminal transactivation domain. *ΔNp73* is overexpressed in CRC, and its upregulation is a predictor of aggressiveness, recurrence, chemoresistance, and poor prognosis in patients diagnosed with most tumor types, including CRC [11]. Interestingly, *ΔNp73* is packaged in exosomes and promotes cancer progression and might therefore be essential in the communication between tumor and stroma [12]. ΔNp73 might exert its oncogenic potential through the modulation of a wide range of effectors involved in various pro-tumoral pathways, such as lymphangiogenesis, vasculogenesis, and metastasis [13]. Various proteins involved in cell adhesion, such as *MSN*, *CALR*, *SRC*, *DSG2*, *DSC3*, *LGALS3BP*, and *ITGB4*, have been found to be upregulated by *ΔNp73*, whereas *TLN1*, *CDH3*, *PTPRF*, *PDCD6IP*, and *COL6A1* are downregulated by *ΔNp73*. The dysregulation of proteins (e.g. *PES1*, *NGDN*, *IMP3*, *SURF6*, *NME1*, and *ZEB1*) associated with the tumorigenesis process, prognosis, and treatment resistance has also been associated with aberrant *ΔNp73* overexpression [13,14]. Remarkably, numerous drugs that activate or block the tumor suppressor/oncogenic functions of various *TP53* family members, including *ΔNp73*, have been identified [15]. With this background information, we decided to explore the involvement of *ΔNp73* in CRC-PM.

Materials and methods

Cell cultures and *ΔNp73* stable transfection

HCT116 human colon cancer cells obtained from the American Type Culture Collection (ATCC, Manassas, VA, USA) were grown in Dulbecco's modified Eagle's medium (DMEM; Corning, Catalog No. 10-013-CVR, New York, NY, USA), supplemented with 10% heat-inactivated fetal bovine serum (FBS; Corning Catalog No. 35-079-CV), 2 mM L-glutamine (Gibco, Catalog No. 2503030-081, Waltham, MA, USA), 1% penicillin/streptomycin stock solution (P/S; Corning, Catalog No. 30-009-CI), and amphotericin B (0.25 µg/ml; Corning). Primary human mesothelial cells purchased from Innoprot (P10770; Bizkaia, Spain) were cultured in p100 plates coated with Collagen I-Cell Culture Surface Coating Kit (Innoprot P8188) in mesothelial cell medium (Innoprot P60167). HCT116 cells were stably transfected with pEF1a-IRES-GFP (HCT116-mock) or pEF1a-ΔNp73β-IRES-GFP (HCT116-ΔNp73) plasmids (generously provided by Dr. Marín and Dr. Marqués from the Biomedical Institute, University of León, Spain [16]) using Lipofectamine 2000 (Thermo Fisher Scientific, Waltham, MA, USA), following the manufacturer's instructions. ΔNp73β is an amino-terminal truncated variant that also lacks exon 13 and has been reported to transactivate its target genes more efficiently that other *ΔNp73* isoforms [17]. Cells overexpressing *ΔNp73* and control cells were selected by sorting using green fluorescent protein as a marker.

Isolation of extracellular vesicles from culture medium

When 80% confluence was reached, 10^5 HCT116-ΔNp73 and HCT116-mock transfected cells were seeded. The supernatant was collected and centrifuged for 15 min at 1,500 × *g*. To pellet the extracellular vesicles (EVs), the supernatant was then ultracentrifuged at 17,000 × *g* in ultra-clear centrifuge tubes (Beckman Coulter, Indianapolis, IN, USA) for 30 min and filtered through 0.22-µm Millipore syringe filters. The supernatant was then ultracentrifuged at 120,000 × *g* for 70 min. The supernatant was then discarded, and the pellet containing EVs was resuspended in 200 µl of sterile PBS and stored at −80 °C for later use [12].

Mesothelial-to-mesenchymal transition evaluation

Conditioned medium was collected from the initial 10^6 HCT116-ΔNp73 and HCT116-mock cell cultures when 80% confluence was reached. The conditioned medium was mixed at a ratio of 75/25 with mesothelial cell culture medium. Human mesothelial cells (Innoprot P10770) were cultured in p100 plates coated with COL1 Cell Culture Surface Coating Kit (Innoprot P8188) in mesothelial cell medium (Innoprot P60167). After 24 h, the conditioned mixed medium was added. Replacement of the conditioned medium was repeated every 48 h, checking cell viability. The assay was maintained for 144 h; the RNA was then extracted to analyze epithelial/mesothelial-to-mesenchymal transition (EMT/MMT) gene expression. The primers are listed in supplementary material, Table S1.

Extracellular matrix (ECM) cell adhesion experiments

The Chemicon® ECM Cell Adhesion Array Kit (Merck KGaA, Darmstadt, Germany; Catalog No. ECM540) containing the ECM proteins COL1, COL2, COL4, FN1, LAM, TN, and VN was employed in ECM cell adhesion experiments. The number of

adherent cells was detected by colorimetry. In brief, the assay consisted of a p96-well plate coated with the aforementioned ECM proteins and seeded with 10^4 HCT116-ΔNp73 or HCT116-mock cells that were allowed to attach. The wells were then washed to remove nonadherent cells, and 100 µl of cell stain solution was added. Binding capacity was quantified with a Spectrophotometer Plate Reader (VersaMax, Molecular Devices Corporation, CA, USA), and absorbance readings were analyzed statistically for each protein comparing HCT116 *ΔNp73* versus control groups.

Orthotopic model of peritoneal metastasis in mice

The mice used in all experiments were 6-week-old female nude/nude athymic mice (Charles River Laboratories, Wilmington, MA, USA). All procedures were approved by the Institutional Body for Animal Welfare (OEBA) and according to European, Spanish, and local regulations [18].

Mice were allocated into two groups ($n = 10$ per group) and injected i.p. with 3×10^5 HCT116-ΔNp73 or HCT116-mock cells. The cell injection was performed in the left iliac fossa with a 25G syringe. The mice were monitored for 15 days and euthanized under anesthesia with isoflurane. Blood was extracted, and plasma was isolated and stored at −80 °C. The abdominal cavity was opened using a xiphopubic incision, exploring the abdominal cavity in search of tumor deposits. The adapted peritoneal carcinosis index (PCI) was calculated by the following method. The mouse abdomen was divided into quadrants; each flank or hemi-diaphragm was assigned a point in case of involvement. The proportion of actual involvement over the theoretical maximum was then calculated and expressed as a percentage. Ascitic fluid, implants, liver, kidney, and lungs were extracted and stored at −80 °C for further study.

Orthotopic model of peritoneal metastasis in mice with exposure to EVs

EVs were isolated from HCT116-ΔNp73 and HCT116-mock cell culture medium as previously described. EV i.p. injection was performed at the left iliac fossa ($n = 10$, per group) with a 25G syringe. Inoculations were performed every 72 h, for 10 rounds. At the end of the conditioning protocol, 3×10^5 HCT116 cells were injected i.p., and i.p. injection of EVs continued over 16 days, then the mice were euthanized under isoflurane anesthesia. Blood was extracted and plasma was isolated and stored at −80 °C. The abdominal cavity was opened using a xiphopubic incision, exploring the abdominal cavity in search of tumor deposits. Peritoneal involvement was quantified using the previously described simplified mouse PCI, and the liver, lungs, kidneys, peritoneal tumor deposits, and ascitic fluid were collected and stored frozen at −80 °C.

Human sample collection

Tumor metastases, healthy peritoneal tissues, and ascitic fluid were collected from 30 patients diagnosed with CRC-PM between 2017 and 2019 at La Paz University Hospital (Madrid, Spain). Patients were informed and gave their consent to participate in this study following the ethics committee's approval.

Tissue was extracted intraoperatively and stored at −80 °C. Histological confirmation of the samples was performed by our hospital's pathologists. Postoperative follow-up covers the period from January 2017 to May 2022. The following events were registered: relapse, death, overall survival (OS), and disease-free survival (DFS). The participants' characteristics are listed in Table 1.

RNA extraction and RT-qPCR

RNA extraction was performed from cell extracts, solid tissues from patients, and solid tissues from mice using the Easy-RED™ Total RNA Extraction Kit (iNtRON Biotechnology, Seongnam, Republic of Korea) following the manufacturer's instructions. The amount of RNA was quantified in a NanoDrop ND-1000 spectrophotometer (Thermo Fisher Scientific). Reverse transcription

Table 1. Main characteristics of patients with peritoneal carcinosis included in our series.

Characteristic	No. of patients
Sex	30
Female	15
Male	15
Age, years (mean, SD)	62 ± 10.9
PCI (mean, SD)	13 ± 11.4
Relapse	76%
Type	
Synchronous	16
Metachronous	14
OS, days (mean)	1,100
DFS, days	438
Vascular invasion	
Positive	13
Negative	7
Liver metastasis	
Positive	10
Negative	20
Ascites fluid cytology	
Positive	6
Negative	12
Histology	
Adenocarcinoma	16
Mucinous	4
Colloid	2
Goblet cell	4
Signet ring cell	1
Micropapillary	3
Primary tumor location	
Appendix	9
Right	7
Left	9
Rectum	5

Abbreviations: DFS, disease-free survival; OS, overall survival; PCI, peritoneal carcinosis index; SD, standard deviation.

synthesis of cDNA was performed using 400 ng RNA using the Transcriptor cDNA Synthesis Kit (Roche Diagnostics, Basel, Switzerland) in a thermocycler. Gene expression was checked by quantitative polymerase chain reaction using a LightCycler-FastStart DNA Master SYBR Green I Kit (Roche Diagnostics) on a Light Cycler apparatus (Roche Diagnostics). Each reaction was performed in a final volume of 20 µl, containing 2 µl cDNA. *GAPDH* was employed as the reference transcript. Expression levels in the participants were calculated as the ratio of the target gene transcript in the tumor tissue to the healthy tissue, normalized to the expression of the reference transcript using the equation described by Livak *et al* [19] ($2^{-\Delta\Delta Ct}$ Method). We analyzed the expression of the following genes associated with the EMT/MMT: *ZEB1*, *CDH1*, *FN1*, *VIM*, and *TWIST1*. Expression levels of *ΔNp73* and its putative target effectors *MSN*, *ITGB4*, *SNAI1*, and *PES1* were evaluated in the human and mouse samples. Supplementary material, Table S1 lists the primer sequences used.

Western blotting

For western blots, 60 µg solid sample was homogenized, processed with radioimmunoprecipitation assay (RIPA), and stored at −80 °C. The amount of protein was quantified using the Pierce Micro BCA Protein Assay Kit (Thermo Fisher Scientific). To check each sample's viability, 5 µg protein was used in 10% sodium dodecyl-sulfate polyacrylamide gel electrophoresis (SDS/PAGE) and Coomassie Blue staining. Western blots were then performed by transferring proteins onto nitrocellulose membranes (Hybond-C extra; GE-Healthcare, Chicago, IL, USA) at 100 V for 90 min. After blocking for 1 h, the membranes were incubated with primary antibody against MSN (Sigma-Aldrich Ref. No. HPA-011135). Bands were analyzed using Fiji software (https://imagej.net/software/fiji/downloads, 2023), with GAPDH as the loading control. MSN overexpression was calculated after normalization with GAPDH band intensity values. Statistical significance was calculated using Student's *t*-test, considering as significant p values <0.05.

Statistical analyses

The expression levels of *ΔNp73* and its target genes were divided according to the median. The DFS analysis did not include the patients with pathologic stage IV disease. The DFS and OS distribution was estimated by the Kaplan–Meier method [12]. The correlation between gene expression levels was assessed using Pearson's correlation test. For the statistical study of the mouse models, the adhesion assay, changes in the mesothelial cell expression levels, and associations between clinical parameters and target gene expression levels, we calculated the mean and standard deviation and performed Student's *t*-test. All p values were two-sided, and values <0.05 were considered to indicate statistical significance. The analyses were conducted using R (Posit Software, PBC, Boston, MA, USA. http://www.posit.co/, version 2023.9.1.494).

Results

ΔNp73 increased implantation capacity of colorectal cancer cells in orthotopic mouse model

Sixteen days after the i.p. injection of HCT116-ΔNp73 and HCT116-mock cells, the mice were euthanized, and an adjusted PCI was calculated. Those mice injected with HCT116-ΔNp73 cells showed an adjusted PCI of 85% (confluent metastasis, involvement of the mesenteric root and abdominal wall, and macroscopic lung metastasis), and those with HCT116-mock cells showed an adjusted PCI of 50% (isolated deposits), supporting the role of *ΔNp73* in promoting peritoneal dissemination. A scheme of the model and representative images of the mice are shown in Figure 1A–D.

Analysis of the mRNA levels of *ΔNp73* and its target genes in tumor deposits from HCT116-ΔNp73 versus control cells revealed a significant *ΔNp73* upregulation of 826.96 ($p = 0.00001$), as expected, and an *ITGB4* upregulation of 1.5 ($p = 0.01$). No change in the expression levels for *MSN* and *ZEB1* were observed (Figure 1E). MSN expression was evaluated at the protein level, observing a 2.8-fold upregulation ($p = 0.00049$) (Figure 1F,G). Taken together, these findings support the role of *ΔNp73* and its effectors as mediators of peritoneal dissemination.

EVs isolated from HCT116-ΔNp73 conditioned medium favored peritoneal implantation in orthotopic mouse model

Given that compounds delivered to the peritoneal fluid by the primary tumor, such as cytokines and EVs, might play a significant role in peritoneal dissemination, we used a mouse model in which mice were injected with EVs from HCT116-ΔNp73 conditioned medium (EVs-ΔNp73) and control cells (EV-mock) every 72 h for 10 rounds before injecting HCT116-mock cells into the mice. We then continued with the same EV inoculation regimen for 16 days, after which the mice were euthanized. The adjusted PCI was 91% (diaphragmatic domes, mesentery, peritoneum, and liver metastasis) for the EVs-ΔNp73 mice and 68% (isolated tumor deposits) for the EV-mock group. A scheme of the model and representative images of the mice are shown in Figure 1H–J.

Interestingly, a 4.8-fold change in mRNA overexpression was observed for *ΔNp73* in the EVs-ΔNp73 group compared with the control mice ($p = 0.00008$), a 2.59-fold change for *MSN* ($p = 0.08$), a 1.77-fold change for *ITGB4* ($p = 0.1$), and a 2.87-fold change for *ZEB1* ($p = 0.04$) (Figure 1K). There was no correlation for MSN at the protein level. The data are shown in Figure 1L,M. The results support the role of EVs from

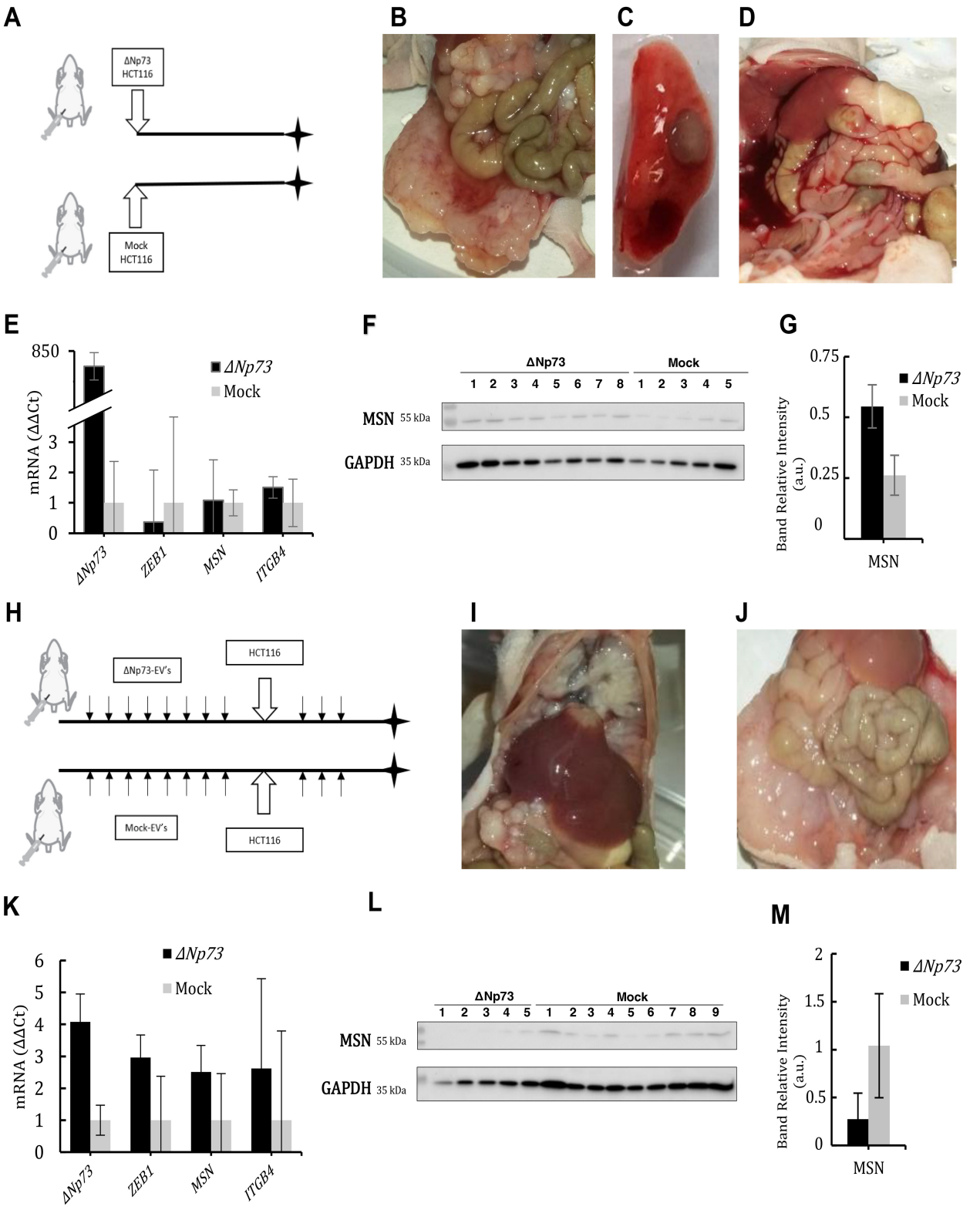

Figure 1. ΔNp73 promotes adhesion of CRC cells to peritoneum in two orthotopic mouse models. (A) Scheme of our first mouse model in which nude mice were i.p. injected with HCT116-ΔNp73 and HCT116 mock cells and sacrificed at day 16. (B) Representative images of affected peritoneum of mouse injected with HCT116-ΔNp73 cells showing confluent metastasis, involvement of mesenteric root and abdominal wall, and (C) macroscopic lung metastasis. (D) Representative image of isolated tumor deposits. (E) mRNA expression levels of *ΔNp73*, *ZEB1*, *MSN*, and *ITGB4* in mouse tumor deposits. (F) Protein levels of MSN in tumor deposits and (G) their quantification. (H) Scheme of our second orthotopic mouse model in which mice were injected i.p. with isolated EVs from HCT116-ΔNp73 cells and EVs from HCT116-mock cells. Injection of EVs was performed every 72 h for 10 rounds, followed by inoculation with HCT116-mock cells. Subsequently, injection of EVs continued every 72 h until euthanasia on day 21 after cell injection. (I) Representative images of individual mice injected with EVs from HCT116-ΔNp73 cells showing involvement of diaphragmatic domes, the presence of tumor deposits in the mesentery, peritoneum, and liver metastasis. (J) Representative images of individual mice injected with EVs from HCT116-mock individual cells showing solid tumor deposits; other organs were not affected. (K) mRNA expression levels of *ΔNp73*, *ZEB1*, *MSN*, and *ITGB4* in mice tumor deposits. (L) Protein expression levels of MSN in tumor deposits and (M) its quantification. (A) and (H) created with BioRender.com.

HCT116-*ΔNp73* CRC cells as relevant promoters of peritoneal metastasis.

ΔNp73 is involved in ability of CRC cells to adhere to ECM proteins and promotes MMT

Based on our mouse model results, we proceeded to evaluate whether the *ΔNp73* upregulation in the HCT116-CRC cells modified their ability to adhere to the ECM proteins COL1, COL2, COL4, FN, laminin (LN), and VN. We observed a remarkable increase in the adhesion of HCT116-ΔNp73 compared with HCT116-mock cells, with a 5.85-fold increase for COL1 ($p = 0.039$), a 7.93-fold increase for COL2 ($p = 0.029$), a 4.18-fold increase for FN ($p = 0.032$), and a 3.71-fold increase for LN ($p = 0.003$) (Figure 2A). The mRNA levels in HCT116-ΔNp73 compared with those in the mock controls was 1.66-fold higher for *MSN* ($p = 0.015$), 1.995-fold higher for *ITGB4* ($p = 0.008$), and 1,041-fold higher for *ΔNp73* (Figure 2B). Thus, *ΔNp73* overexpression increases the number of HCT116 CRC cells bound to ECM proteins.

The MMT process has been involved in the implantation of CRC cells in the peritoneum. Sandoval *et al* [10] reported that areas with tumor deposits are enriched in CAFs that might be derived from resident mesothelial cells. These CAFs might secrete factors that promote the disorganization of the peritoneum, making it more accessible for tumor cells. Given that, in our orthotopic mouse model, EVs-ΔNp73 increased the number of CRC cells bound to the peritoneum, we explored whether the conditioned medium from HCT116-ΔNp73 would modify the phenotype of primary mesothelial cells and their expression pattern compared with HCT116-mock cells. Thus, we studied changes in the expression levels of the EMT- and MMT-associated markers *CDH1*, *FN1*, *VIM*, *SNAI1*, *TWIST1*, and *ZEB1*. The expression levels of *ΔNp73* and its putative target genes, *MSN* and *ITGB4*, were also evaluated (Figure 2C). We observed a surprising downregulation of *MSN* (0.4-fold change) and *SNAI1* (0.35-fold change) and overexpression of *ZEB1* (3.74-fold change) and *CDH1* (2-fold change) in the mesothelial cells exposed to conditioned medium from HCT116-ΔNp73. No significant changes were observed for *ITGB4*, *VIM*, *FN1*, or *TWIST1*. *ΔNp73* was undetectable in the primary mesothelial cells. Next, we evaluated changes in the phenotype of mesothelial cells exposed to conditioned medium with respect to control medium (Figure 2D–F). We observed that the phenotype of mesothelial cells exposed to conditioned medium from HCT116-mock cells varied minimally (Figure 2E). By contrast, conditioned medium from HCT116-ΔNp73 cells confers a mesenchymal phenotype to primary mesothelial cells (Figure 2F).

In summary, *ΔNp73* cells might secrete various compounds, including cytokines and EVs, which might promote tumor cell implantation by inducing significant changes in the mesothelial layer.

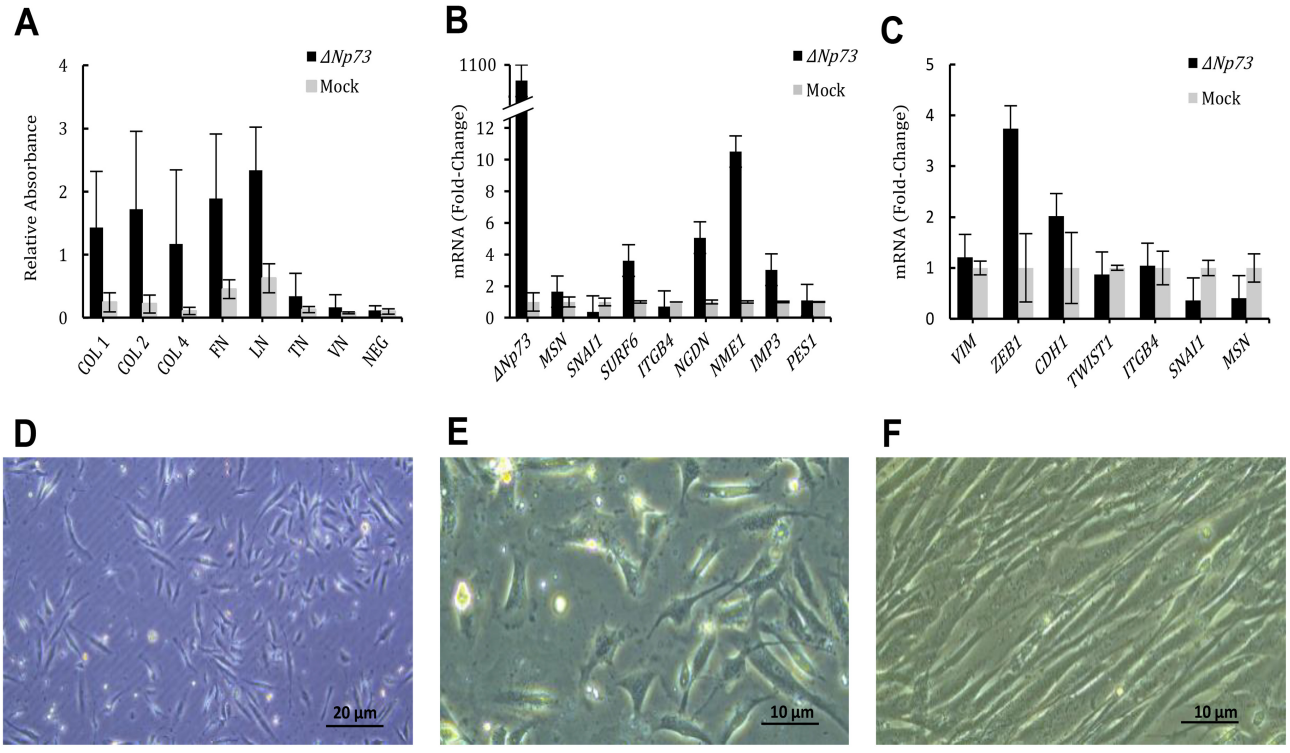

Figure 2. ΔNp73 promotes adhesion to ECM proteins, the induction of its effector targets, and a mesenchymal phenotype. (A) The adhesion assay showed more HCT116-ΔNp73 cells than control cells adhered to various ECM proteins. HCT116-ΔNp73 cells showed higher expression of (B) ΔNp73 putative target genes and (C) mesothelial-to-mesenchymal-related genes. Primary mesothelial cells exposed to (D) mesothelial cell culture medium, (E) conditioned medium from HCT116-mock cells, and (F) HCT116-ΔNp73 cells, respectively, for 144 h.

MSN and *ITGB4* predict prognosis of patients with CRC and peritoneal metastasis

The overexpression of *ΔNp73* has been associated with a poor prognosis in most tumor types, including CRC [11]. The current study evaluated the expression levels of *ΔNp73* and its putative effectors *MSN*, *ITGB4*, *SNAI1*, and *PES1* in tumor metastasis and healthy mesothelial tissues from a series of 30 patients diagnosed with CRC-PM, as well as their association with various clinical-pathological tumor characteristics and the patients' DFS and OS. The patients' characteristics are listed in Table 2, and their DFS and OS are shown in Figure 3A,B. The Kaplan–Meier survival curves showed that those patients with a PCI >10 presented lower OS ($p = 0.007$) and DFS ($p = 0.001$), indicating that PCI is a good prognostic predictor (Figure 3C,D). Unexpectedly, no correlation regarding *ΔNp73* expression levels was observed, for either OS or DFS (Figure 3E,F). However, the Kaplan–Meier survival analysis revealed that patients with high *ITGB4* levels relative to the median had a lower DFS ($p = 0.009$) (Figure 3G). A trend was observed for OS and *MSN* expression ($p = 0.08$); patients with high *MSN* levels relative to the median had a lower OS ($p = 0.08$) (Figure 3H).

The expression levels of *ΔNp73*, *MSN*, *ITGB4*, *SNAIL1*, and *PES1* were categorized based on the PCI, with the relative expression of *ΔNp73* and *ITGB4* mRNA being upregulated in the tumor tissue compared with the healthy peritoneum tissue (ΔΔCt values are listed in Table 2). When we evaluated the correlation between these genes' mRNA levels and the tumors' clinical-pathological characteristics, we observed that the upregulation of *MSN* and *SNAI1* was associated with liver metastasis [2.42-fold change ($p = 0.030$) and 2.338-fold change ($p = 0.039$), respectively] (Figure 3I,J) and that *ITGB4* overexpression was associated with vascular invasion [2.49-fold change ($p = 0.02$)] (Figure 3K).

Next, we analyzed the correlation between *ΔNp73* and its effectors (Figure 3L–P). Direct correlations were obtained for *PES1* and *ΔNp73* ($R = 0.43$; $p = 0.039$) (Figure 3L), *SNAI1* ($R = 0.43$; $p = 0.034$) (Figure 3M), and *MSN* ($R = 0.65$; $p = 0.0005$) (Figure 3N); and *MSN* and *ΔNp73* ($R = 0.5$; $p = 0.014$) (Figure 3O), and *SNAI1* ($R = 0.74$; $p = 0.00003$) (Figure 3P).

Discussion

This study showed that *ΔNp73*, an oncogenic member of the TP53 family, and its putative effector targets were involved in CRC-PC and could be employed as prognostic markers of the disease. In an orthotopic carcinosis model in mice, we observed that CRC cells that upregulated *ΔNp73* showed higher binding capacity to the peritoneum than control cells, presenting a significantly higher adjusted PCI and upregulation of the putative *ΔNp73* effector *MSN*. Similar findings were obtained in an orthotopic model using CRC cells treated with EVs with high *ΔNp73* content. Evs secreted by the primary tumor into the peritoneal cavity play a key role in tumor cell implantation. Interestingly, *ΔNp73* was overexpressed in the peritoneal implants of mice treated with EVs with high *ΔNp73* content, which demonstrates that this oncogenic variant is transferred from EVs to cancer cells and promotes peritoneal metastasis. In both models, the *ΔNp73* putative effector targets, *MSN*, *ITGβ4*, and *ZEB1* [14], involved in cell adhesion were upregulated in the mouse implants.

The involvement of *ΔNp73* in adhesion processes was validated in an adhesion assay where those CRC cells overexpressing *ΔNp73* attached with higher avidity to the ECM proteins COL1, COL2, FN, and LN. The *ΔNp73*-overexpressing cells also showed alteration of various putative *ΔNp73* effectors involved in various disease progression stages, including adhesion and chemoresistance [20]. *MSN*, *SURF6*, *NGDN*, *NME1*, *IMP3*, and *PES1* were therefore upregulated, whereas *SNAI1* and *ITGB4* were downregulated.

MMT is essential in peritoneal metastasis [21]; we therefore exposed mesothelial cells to the conditioned medium of *ΔNp73*-overexpressing cells and control cells. Interestingly, we observed a significant mesenchymal phenotype in those cells exposed to the conditioned medium of *ΔNp73*-upregulating cells that was accompanied by significant upregulation of *ZEB1* and *CDH1*, and downregulation of *MSN* and *SNAI1* ΔNp73 was previously identified as crucial in EMT in various physiological contexts [22]; however, its involvement in MMT has not been reported. Lenos *et al* [8] reported MSN upregulation in patients with CRC-PC and associated it

Table 2. RT-qPCR values obtained from human samples adjusted by peritoneal carcinosis index (PCI). Ct values are after normalization to *GAPDH* ($Ct_{target} - Ct_{norm}$) for both healthy and tumor tissue; ΔΔCt is calculated using healthy tissue as control for each patient ($\Delta\Delta Ct = \Delta Ct_T - \Delta Ct_H$). Values show marked relative overexpression of Δ*Np73* and *ITGB4* in tumoral tissue (PCI > 10 and PCI < 10).

Gene	PCI	Healthy tissue (ΔCt_H)	Tumor tissue (ΔCt_T)	mRNA expression ($2^{-\Delta\Delta Ct}$)
ΔNp73	>10	12.66 ± 3.22	13.40 ± 2.36	14.80 ± 38.09
	<10	11.47 ± 4.96	12.33 ± 3.33	2.57 ± 4.37
MSN	>10	0.82 ± 1.79	2.88 ± 1.66	0.49 ± 0.54
	<10	0.56 ± 1.42	2.79 ± 2.28	0.50 ± 0.52
ITGB4	>10	4.97 ± 2.89	3.67 ± 1.90	5.70 ± 14.66
	<10	5.77 ± 1.22	6.17 ± 2.34	4.43 ± 9.24
SNAI1	>10	3.95 ± 2.88	5.78 ± 2.08	0.59 ± 0.76
	<10	3.84 ± 1.52	6.31 ± 2.50	0.66 ± 0.71
PES1	>10	3.18 ± 1.96	4.56 ± 2.50	0.61 ± 0.99
	<10	2.13 ± 2.21	3.30 ± 3.46	1.08 ± 1.45

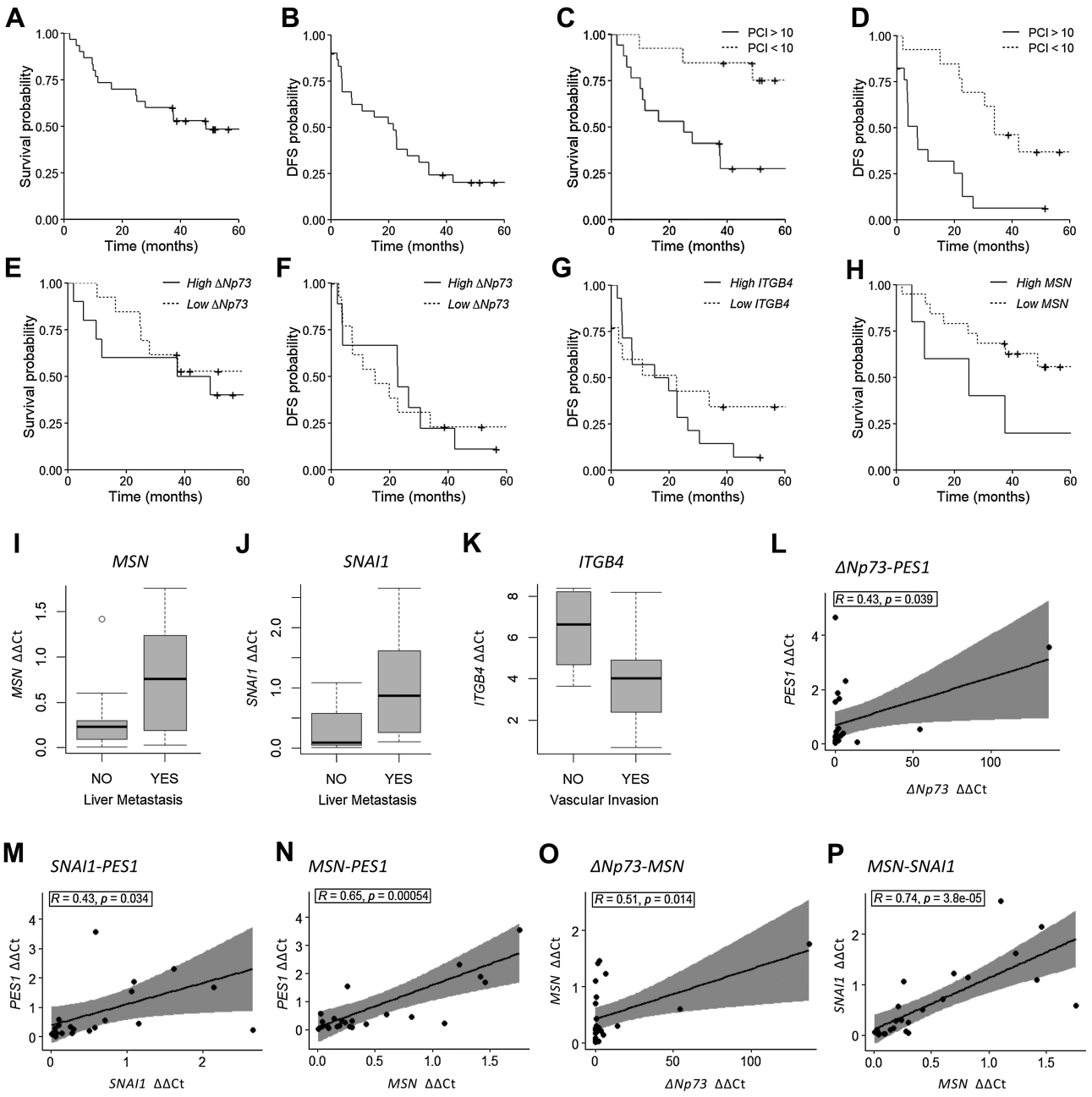

Figure 3. Patients with peritoneal carcinosis (CRC-PC). (A) OS and (B) DFS in series of 30 patients diagnosed with CRC-PM. (C) OS and (D) DFS stratified according to PCI ≤10 ($p = 0.001$ and $p = 0.007$, respectively). (E) OS and (F) DFS with respect to Δ*Np73* expression levels (no statistical significance). (G) High *ITGB4* levels are associated with DFS ($p = 0.009$). (H) High *MSN* levels are associated with OS ($p = 0.08$). (I) High levels of *MSN* and (J) *SNAI1* in metastasis versus healthy peritoneal tissue, respectively, were associated with liver metastasis. (K) High *ITGB4* levels in tumor metastases were associated with vascular invasion; a direct correlation was observed between (L) *ΔNp73* and *PES1*, (M) *PES1* and *SNAI1*, (N) *MSN* and *PES1*, (O) *ΔNp73* and *MSN*, and (P) *MSN* and *SNAI1*.

with the CSM4 mesenchymal subtype. We postulate *ΔNp73* as the master regulator of MSN and other proteins involved in adhesion and progression to the peritoneum, although further studies are required to accurately understand the exact mechanism. The involvement of ΔNp73 in the EMT process might therefore facilitate the detachment of CRC cells from the primary tumor and their release to the peritoneal fluid. The primary tumor might also secrete EVs to the peritoneal cavity, promoting the restructuring of the mesothelium and favoring the adhesion of cancer cells to the peritoneum, a process in which MMT might be critical. Furthermore, *ΔNp73*-overexpressing cells might induce the expression of its target gene, ITGB4, a protein involved in adhesion to the ECM through its receptor laminin and associated with the attachment of tumor cells to the peritoneum. In our mouse models, EVs induced the *MSN* expression reported to be present in mesothelial cells as part of the ezrin/radixin/moesin complex involved in the regulation of cell adhesion, polarity, and migration by cross-linking between the actin cytoskeleton and the plasma membrane [23].

As expected, a higher PCI in our series of 30 patients was associated with shorter DFS and OS. However, there was no association between *ΔNp73* expression and DFS and OS, which could be due to the fact that all of our patients were at stage IV. Larger series are needed to evaluate whether the *ΔNp73* expression levels differ in stage IV patients with peritoneal metastasis with differing outcomes. Interestingly, we found statistically significant correlations between the expression levels of *ΔNp73* and *MSN* and *PES1*, of *SNAI1* and *MSN* and *PES*, and of *MSN* and *PES*, supporting the concept that *ΔNp73* might also be regulating its target genes in patients. High levels of *MSN* and *SNAI1* were also associated with liver metastasis, while low *ITGB4* levels were associated with vascular invasion, which is in line with our previous results showing that *ΔNp73* effectors might predict the prognosis of patients more accurately than *ΔNp73* [11]. Those patients who had higher levels of *MSN* and *ITGB4* had shorter DFS and OS. *MSN* and *ITGB4* could therefore be employed in the clinical setting as prognostic biomarkers. Our results support the findings published by Lenos *et al* [8] that identified *MSN* as a critical player in peritoneal dissemination and that CRC-PC represents the molecular subtype CMS4. As discussed above, the conditioned medium of CRC cells upregulating *ΔNp73* elicits a mesenchymal phenotype, which agrees with the results of Lenos *et al* [8]. Unfortunately, we did not have the data regarding the molecular subtype in our series to confirm that those tumors upregulating *ΔNp73* and *MSN* are of the CSM4 subtype.

In conclusion, further studies are needed to evaluate whether *ΔNp73* can predict metachronous PM development. With this aim in mind, it would be interesting to participate in the HIPECT4 [24] clinical trial, which tests the prophylactic use of HIPEC. The evaluation of *ΔNp73* expression levels in these patients would provide valuable information regarding the involvement of this isoform in peritoneal metastasis. Remarkably, a wide variety of compounds that block the pro-tumoral activity of *ΔNp73* have been identified [25]. Given that the chemotherapy agents employed in HIPEC do not confer benefits to CRS [5], our data provide a new promising targetable pathway for patients with CRC-PC.

Acknowledgements

This study was funded by the Carlos III Health Institute (ISCIII) through projects PI18/00473 and PI21/01047 co-funded by European Union (FEDER funds). We would like to thank Marina Arranz Álvarez (Biobanco IdiPAZ) for her contribution to human sample collection and the Production Department of Hospital La Paz for the support with the English version.

Author contributions statement

DP-M participated in human sample recruitment and processing, performed experiments and participated in data collection, data analysis, data interpretation, literature search, generation of figures and writing of the manuscript. LA-M performed experiments and participated in data collection, data analysis and data interpretation. MG-A performed experiments and participated in data analysis and data interpretation. RR-G performed experiments and participated in data collection, data analysis and data interpretation. PC performed experiments and participated in data collection. NR and JPP-R participated in the recruitment of human samples. RB participated in data analysis and data interpretation. IP-N led the recruitment of human samples, participated in data interpretation and writing of the manuscript and supervision of the project. GD conceived of the experiments and participated in sample processing, data collection, data analysis, data interpretation, literature searching, writing the manuscript and supervision of the project. All authors gave final approval of the submitted and published versions.

Data availability statement

The data that support the findings of this study are available from the corresponding author upon reasonable request.

References

1. Sung H, Ferlay J, Siegel RL, *et al*. Global cancer statistics 2020: GLOBOCAN estimates of incidence and mortality worldwide for 36 cancers in 185 countries. *CA Cancer J Clin* 2021; **71:** 209–249.
2. Cervantes A, Adam R, Roselló S, *et al*. Metastatic colorectal cancer: ESMO clinical practice guideline for diagnosis, treatment and follow-up. *Ann Oncol* 2023; **34:** 10–32.
3. Brierley J, Gospodarowicz MK, Wittekind C. *TNM classification of malignant tumours* (8th edn). John Wiley & Sons, Inc.: Oxford, Hoboken, 2017.
4. Mirnezami R, Mehta AM, Chandrakumaran K, *et al*. Cytoreductive surgery in combination with hyperthermic intraperitoneal chemotherapy improves survival in patients with colorectal peritoneal metastases compared with systemic chemotherapy alone. *Br J Cancer* 2014; **111:** 1500–1508.
5. Quénet F, Elias D, Roca L, *et al*. Cytoreductive surgery plus hyperthermic intraperitoneal chemotherapy versus cytoreductive surgery alone for colorectal peritoneal metastases (PRODIGE 7): a multicentre, randomised, open-label, phase 3 trial. *Lancet Oncol* 2021; **22:** 256–266.
6. Morgan RB, Dhiman A, Sood D, *et al*. Mutational profiles and prognostic impact in colorectal and high-grade appendiceal adenocarcinoma with peritoneal metastases. *J Surg Oncol* 2023; **127:** 831–840.
7. Lee JH, Ahn BK, Baik SS, *et al*. Comprehensive analysis of somatic mutations in colorectal cancer with peritoneal metastasis. *In Vivo* 2019; **33:** 447–452.
8. Lenos KJ, Bach S, Ferreira Moreno L, *et al*. Molecular characterization of colorectal cancer related peritoneal metastatic disease. *Nat Commun* 2022; **13:** 4443.
9. Lepsenyi M, Algethami N, Al-Haidari AA, *et al*. CXCL2-CXCR2 axis mediates αV integrin-dependent peritoneal metastasis of colon cancer cells. *Clin Exp Metastasis* 2021; **38:** 401–410.

10. Sandoval P, Jiménez-Heffernan JA, Rynne-Vidal Á, *et al*. Carcinoma-associated fibroblasts derive from mesothelial cells via mesothelial-to-mesenchymal transition in peritoneal metastasis. *J Pathol* 2013; **231:** 517–531.
11. Soldevilla B, Díaz R, Silva J, *et al*. Prognostic impact of ΔTAp73 isoform levels and their target genes in colon cancer patients. *Clin Cancer Res* 2011; **17:** 6029–6039.
12. Soldevilla B, Rodríguez M, Millán CS, *et al*. Tumor-derived exosomes are enriched in ΔNp73, which promotes oncogenic potential in acceptor cells and correlates with patient survival. *Hum Mol Genet* 2014; **23:** 467–478.
13. Garranzo-Asensio M, Rodríguez-Cobos J, San Millán C, *et al*. In-depth proteomics characterization of ΔNp73 effectors identifies key proteins with diagnostic potential implicated in lymphangiogenesis, vasculogenesis and metastasis in colorectal cancer. *Mol Oncol* 2022; **16:** 2672–2692.
14. Domínguez G, Peña C, Silva J, *et al*. The presence of an intronic deletion in p73 and high levels of ZEB1 alter the TAp73/DeltaTAp73 ratio in colorectal carcinomas. *J Pathol* 2006; **210:** 390–397.
15. Millán C, Soldevilla B, Martín P, *et al*. β-cryptoxanthin synergistically enhances the antitumoral activity of oxaliplatin through ΔNP73 negative regulation in colon cancer. *Clin Cancer Res* 2015; **21:** 4398–4409.
16. Martin-Lopez M, Maeso-Alonso L, Fuertes-Alvarez S, *et al*. p73 is required for appropriate BMP-induced mesenchymal-to-epithelial transition during somatic cell reprogramming. *Cell Death Dis* 2017; **8:** e3034.
17. Domínguez G, García JM, Peña C, *et al*. DeltaTAp73 upregulation correlates with poor prognosis in human tumors: putative in vivo network involving p73 isoforms, p53, and E2F-1. *J Clin Oncol* 2006; **24:** 805–815.
18. de Cuba EM, Kwakman R, van Egmond M, *et al*. Understanding molecular mechanisms in peritoneal dissemination of colorectal cancer: future possibilities for personalised treatment by use of biomarkers. *Virchows Arch* 2012; **461:** 231–243.
19. Livak KJ, Schmittgen TD. Analysis of relative gene expression data using real-time quantitative PCR and the 2(-Delta Delta C(T)) method. *Methods* 2001; **25:** 402–408.
20. Rodríguez N, Peláez A, Barderas R, *et al*. Clinical implications of the deregulated TP73 isoforms expression in cancer. *Clin Transl Oncol* 2018; **20:** 827–836.
21. Pascual-Antón L, Cardeñes B, Sainz de la Cuesta R, *et al*. Mesothelial-to-mesenchymal transition and exosomes in peritoneal metastasis of ovarian cancer. *Int J Mol Sci* 2021; **22:** 11496.
22. Zhang Y, Yan W, Jung YS, *et al*. Mammary epithelial cell polarity is regulated differentially by p73 isoforms via epithelial-to-mesenchymal transition. *J Biol Chem* 2012; **287:** 17746–17753.
23. Kobori T, Tanaka C, Tameishi M, *et al*. Role of ezrin/radixin/moesin in the surface localization of programmed cell death ligand-1 in human colon adenocarcinoma LS180 cells. *Pharmaceuticals (Basel)* 2021; **14:** 864.
24. Arjona-Sánchez A, Barrios P, Boldo-Roda E, *et al*. HIPECT4: multicentre, randomized clinical trial to evaluate safety and efficacy of hyperthermic intra-peritoneal chemotherapy (HIPEC) with mitomycin C used during surgery for treatment of locally advanced colorectal carcinoma. *BMC Cancer* 2018; **18:** 183.
25. Slade N, Horvat A. Targeting p73-a potential approach in cancer treatment. *Curr Pharm Des* 2011; **17:** 591–602.

SUPPLEMENTARY MATERIAL ONLINE

Table S1. Primer sequences used